

2010 GCEP Report

Project title: Self-sorting of Carbon Nanotubes for High Performance Large Area Transparent Electrodes for Solar Cells

Investigators

Zhenan Bao, Associate Professor, Chemical Engineering
Melburne LeMieux, Postdoc Researcher; Soumendra Barman, Michael Vosgueritchian, Graduate Researchers, Jaeyeon Baek, Undergraduate Researcher; Rut Rivera, undergraduate summer internship student

Abstract

Single-Walled Carbon Nanotubes (SWNTs) have superb electronic and mechanical properties; however, SWNTs come in different chiralities making them either metallic (MET) or semiconducting (SC). It is desirable to have only one type in electronic applications. We have recently developed a method to selectively separate the SC and MET SWNTs and form self sorted networks of each on different functionalized surfaces.

In order to deposit the SWNTs, they need to be purified and dispersed into solutions. Here, we systematically vary the dispersion conditions used to disperse SWNTs in solution and then use deposit films onto functionalized substrates resulting in sub-monolayer SWNT networks. We used field effect transistors (FETs) to evaluate the electronic properties of the networks. We show that changing the solution processing conditions changes the properties of SWNTs in solution, the length of SWNTs and the metallic and semiconducting fractions of SWNTs adsorbed on the surface. For optimal SWNTs transistor networks with high on/off ratio, and long unbundled SWNTs a short sonication time is required. However, comparable length and electronic performance can be obtained with increased yield with a slightly longer time. Longer sonication times reduce the length of the SWNTs and degrade the on/off ratio of self sorted SWNT networks by introducing defects, shortening the SWNTs and degrading the solvent.

Recent exploitations of the superior mechanical and electronic properties of carbon nanotubes (CNTs) have led to exciting opportunities in low-cost, high performance, carbon-based electronics. We have incorporated CNT films onto chemically modified polymer layers using both rigid and flexible substrates. We overcame adhesion and roughness issues to fabricate robust CNT films on polymers that are stable even underwater. Organized, high-performance CNT films on polymers enables integration into large area, flexible, solution processable solar cells where they can function as the electrode material in these applications.

The mechanism of SWNT adsorption on a surface is also presented. The chirality, density, and alignment of the SWNTs were heavily influenced by adsorption onto amine functionalized surfaces that were exposed to varying pH solutions, as evidenced by atomic force microscopy (AFM) and Raman spectroscopy. This pH treatment altered the charge density on the surface, allowing for the examination of the contribution from electrostatic interaction to SWNT adsorption and SWNT characteristics. Secondary and tertiary amines with methyl substitutions

were utilized to confirm that adsorption and chirality specific adsorption is largely due to the nitrogen lone pair, not the neighboring hydrogen atoms. Thus, the nature of adsorption is predominantly electrostatic and not due to Van der Waals forces or localized polarization on the SWNTs.

In order to produce these films on different surface and explore their effects, an optimized dry transfer method was developed. This enables SWNT films to be transferred from a surface that allows for controllable deposition of SWNT films to surfaces that normally do not. Thin film transistors (TFT) characteristics, corroborated with μ -Raman spectroscopy, show that by using different surface chemistries, such as with self assembled monolayers (SAMs), it is possible to permanently alter the electronic properties of SWNT films.

We have also developed a novel route to increase the conductivity and reliability of SWNT networks by using a dopant that has a stronger binding energy to SWNTs (stable up to 200 °C), resulting in conductivity values routinely lower than 100 Ω/\square , with transparency higher than 90%, making this a very competitive alternative to ITO.

Finally, we continued investigation of the carbon nanotube/conjugated polymer composite transparent electrodes by studying their properties and investigating their suitability for use in practical, flexible organic electronics applications. In particular, we determined that the nanotube/polymer composites as spin-coated onto flexible substrates are robust under pressure and strain. We also developed a method of patterning these composites directly from solution onto substrates of interest, with feature resolution down to at least 3 microns and nanotube densities sufficient to drive high-performance organic semiconductor devices. Finally, we began a collaborative project to better understand charge transport in large-bundle nanotube networks using nanoscale 4-probe measurements.

Introduction

The application of carbon nanotubes (CNT) to the fabrication of transparent conductive electrodes (TCE) for photovoltaic applications has been investigated in the recent years for their potential to address some of the shortcomings of current Indium-Tin-Oxide (ITO) technologies, namely the high material and fabrication costs and the brittleness of the deposited layers. Their excellent charge-transport properties are particularly suitable for applications relating to display drivers, photovoltaics, and circuits. CNTs have the prospect to meet low fabrication cost targets for the low cost of earth-abundant carbon and for their potential to be dispersed into solution for large area coating. Additionally, they have excellent thermal, mechanical, and electrical properties that make them an ideal candidate for TCEs: they are stable at the high temperatures required to process inorganic devices; they have excellent strength and flexibility; and they have an electrical conductivity three orders of magnitude greater than metals like copper.

Despite their potential, state-of-the-art CNT-based TCEs have still poor performance with a sheet resistance more than ten times higher than ITO electrodes at comparable light transmittance (~80%). The key problem in reducing the sheet resistance of CNT-based layers is that as-synthesized CNTs usually contain a mixture of approximately 67% semiconducting CNTs (sc-CNT) and only 33% metallic CNTs (met-CNT), where the difference in electronic

properties depends on the chirality of the nanotubes. Moreover, the ability to tune the alignment and absorption onto surfaces will lead to optimized optoelectronic properties. And finally, a big driver for alternatives to ITO is a dramatic reduction in cost. To facilitate cost-efficient electronics, large area devices will require cheaper materials such as polymers, along with faster, cheaper solution processing rather than high temperature sputtering.

However, accurate (directed) assembly and orientation in a reproducible fashion of SWNTs over large areas remains an unsolved issue. We have spent considerable effort mitigating this problem by fabricating CNT films with tunable and reproducible chirality, alignment, and density through a spin-assembly method from solution on various substrates. This more elegant approach beyond “random CNT networks” leads to better conductivity with higher transparency since with an optimized CNT network, a thinner film is required.

Results

I. Solution Processing Single Walled Nanotubes

In order to facilitate the integration of single walled carbon nanotubes (SWNTs) into transparent conductors and electronic devices they need to be purified and dispersed into solutions. Understanding the effect solution processing steps can have important implications in the design of SWNT films for these electronic applications. We systematically vary the dispersion conditions used to disperse SWNTs in solution and then use deposit films onto functionalized substrates resulting in sub-monolayer SWNT network field effect transistors (FETs) with a range of device properties. Changing the solution processing conditions changes the properties of SWNTs in solution, the length of SWNTs and the metallic and semiconducting fractions of SWNTs adsorbed on the surface. For optimal SWNTs transistor networks with high on/off ratio, and long unbundled SWNTs a short sonication time is required. However, comparable length and electronic performance can be obtained with increased yield with a slightly longer time. Longer sonication times reduce the length of the SWNTs and degrade the on/off ratio of self sorted SWNT networks by introducing defects, shortening the SWNTs and degrading the solvent. This study shows that careful consideration is required for the scalable processing of SWNT electronic devices.

II. Incorporating CNT Films onto Chemically Modified Polymer Layers Using Both Rigid and Flexible Substrates

CNT films were fabricated on poly(4-vinylphenol) (PVP) insulating films that were cross-linked for stability. Organized CNT networks are deposited via spin-coating on top of functionalized PVP. Atomic force micrographs (AFM) of the sorted and aligned nanotube networks on PVP reveal no damage or delamination of the underlying polymer layer. The CNT network deposited on the PVP on a silicon substrate showed high uniformity from AFM analysis at different length scales. The polymer film roughness of 0.3 nm is similar to that of the underlying native silicon oxide. Due to the increased surface roughness of the flexible ITO/PET substrates, the SWNT networks exhibited a reduction in density and alignment when deposited according to the conditions optimized for rigid silicon substrates.

The robustness and durability of our CNT-based films is demonstrated through operation under aqueous conditions. During the electrical characterization in water, the constant bias held low to

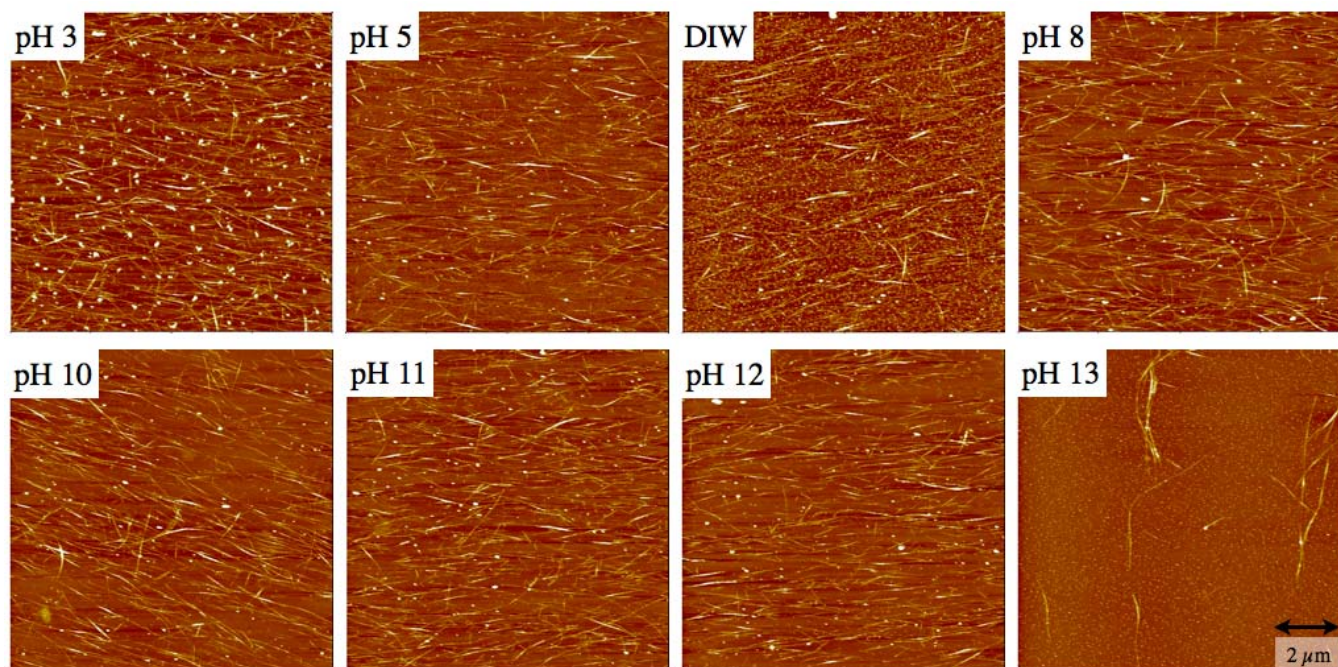
keep the parallel ionic current through the solution to a minimum. The CNT networks were extremely stable in water for over 400 electrical cycles of current. The ability to operate in water is critical for the future development of electronic devices capable of operation in aqueous or complex media.

III. Influence of Electrostatic Interactions on Spin Assembled Single-Walled Carbon Nanotube Networks on Amine Functionalized Surfaces

The electrical current measured is a complete function of the topology of the CNT network adsorbed on the surface. To better understand this, samples were placed in individual vials containing HCl or NaOH solution diluted to each desired pH, ranging from 3 to 13 (Table 1). This produced ammonium-coated surfaces with densities ranging from roughly 3×10^{11} (pH 3) to less than 3×10^4 $\text{NH}_3^+/\text{cm}^2$ (pH 10 and higher). Upon removal from the pH bath, CNT films were spincoated onto the surfaces. Overall, as the pH of the surface was increased from 3 to 13, the density of unmodified CNTs adsorbed on the surface was gradually reduced until approximately pH 12, where at pH 13 the number of tubes adsorbed dropped drastically to almost 0 (per μm^2), as revealed by large scale AFM images (Figure 1). We theorize that as the surface was treated with an aqueous environment at low pH, the amine functional groups convert to cationic ammonium ions. These positive ions likely interacted with the negatively charged carboxylate defect groups on the CNTs in solution.

Table 1: Influence of pH treatment on monolayer properties

Silane	Untreated	pH 3	pH 5	pH 7	pH 8	pH 10	pH 11	pH 12	pH 13
CA (°)	62.3±1.1	-1.9 ±3.4	-0.7 ±1.2	-2.2 ±1.6	-1.3 ±1.0	-1.5 ±2.4	-4.0 ±1.1	-6.6 ±1.4	-24.3 ±2.9
SWE (Å)	6.3±0.4	-0.1 ±0.9	-0.9 ±1.0	-0.7 ±0.8	-0.8 ±0.3	-0.9 ±0.4	-1.8 ±0.3	-3.7 ±0.3	-5.7 ±0.3
NH3+ Density (Theory, cm^{-2})	None	3×10^{11}	3×10^9	3×10^7	3×10^6	3×10^4	N/A	N/A	N/A



	3	5	7	8	10	11	12	13
SWNT Density (μm^{-2})	20.8 ± 2.4	16.4 ± 3.6	17.3 ± 1.4	17.4 ± 1.3	12.8 ± 1.7	12.8 ± 1.5	11.4 ± 1.8	0.3 ± 0.02
Alignment S.D ($^{\circ}$)	41.5 ± 8.2	31.5 ± 5.8	33.6 ± 6.2	29.7 ± 4.1	26.0 ± 2.8	20.9 ± 2.3	23.0 ± 1.1	

Figure 1: AFM topography images of CNT networks on surfaces treated with different pH. With increasing pH, there is a general trend of reduced SWNT density and better alignment. Particles on the surfaces (especially on the pH 3 sample) were a result of impurities in the pH solutions. Note the elimination of a percolating network at pH 13. Z-scale ranges from 0 to 20 nm. At bottom is a summary chart of the AFM data.

At very acidic pHs, the majority of the surface became positively charged. There was a strong electrostatic attraction between this surface and the negatively charged CNTs, leading to high density CNT networks on the surface. Hence, the nanotubes deposited on this highly charged surface were less aligned, and the limited level of alignment observed was a result of the tubes being partially aligned while still in solution.

With increasing pH, the physisorption energy is reduced and the nanotubes are, at least momentarily, less strongly bound to the surface. In this situation, the nanotubes can touch down on the surface and be weakly bound to the surface initially. This allows the nanotube to be better aligned with the fluid flow prior to completely falling to the surface. After the entire length of the tube is in contact with the surface, they are then effectively bound by strong Van der Waals forces. The random tubes deposited on the pH 13 surface are a result of residual fluid drying on

the surface after spinning was stopped and no alignment is observed in these cases. The fact that the alignment can be tuned is important for nanoelectronic devices and nanoscale sensors in which performance is directly affected by CNT topology.

To further elucidate the nature of the surface-SWNT interaction, we repeated the above experiments using the secondary and tertiary amine surfaces. This was used to understand if the steric hindrance of the donating group had any effect in this interaction. We also aimed to determine if the surface-SWNT interaction is primarily between the hydrogen on the amine or the ammonium cation as some simulation results indicated potentially stronger interactions with the hydrogen. In contrast, work by Zhao et al had suggested that, in the gas phase, methyl functional groups could have stronger interactions with SWNTs than amine groups.

Immediately, we observed that the density is much lower on these surfaces for a given pH relative to the primary amine. The steric hindrance from the methyl groups during the surface modification led to lower density. The lower density of amines resulted in the surface ultimately having a lower density of ammonium ions for a given pH. Furthermore, the methyl groups sterically hindered the nanotubes from interacting with the amine lone pair. This methyl group 'buffer' further weakened the electrostatic attraction between the surface and nanotubes. Hence lower CNT densities were obtained overall and nanotubes stopped adsorbing at lower bulk pH values.

Both surfaces yielded the same pH dependence trends of density and alignment as observed on the amine surface. Increasing methyl substitution led to decreasing values of pH where CNT adsorption shutoff takes place. This trend is illustrated in the adsorption curves in Figure 2. Interestingly, the tertiary silane has nearly the same trend line as the amine regarding decrease in CNT versus pH. However, the secondary silane is relatively insensitive to pH changes until shutoff. Importantly, there are no studies carried out on characterizing the surface properties of these silanes, thus the configuration of the functional end group is not known. However, based on contact angle measurements where the secondary amine was always consistently higher, we submit that the methyl group of the secondary amine may be more exposed to the surface, thus limiting this pH response sensitivity. On the other hand, the amine on the tertiary silane is more sterically hindered and less able to interact with the CNTs, as the magnitude of CNT adsorption is the lowest with this system (Figure 2). Similar to the amine monolayers, these surfaces experienced minor etching from pH 10 to 12 treatments, but were still mostly intact. Therefore, shutoff was not a result of the complete removal of the monolayer.

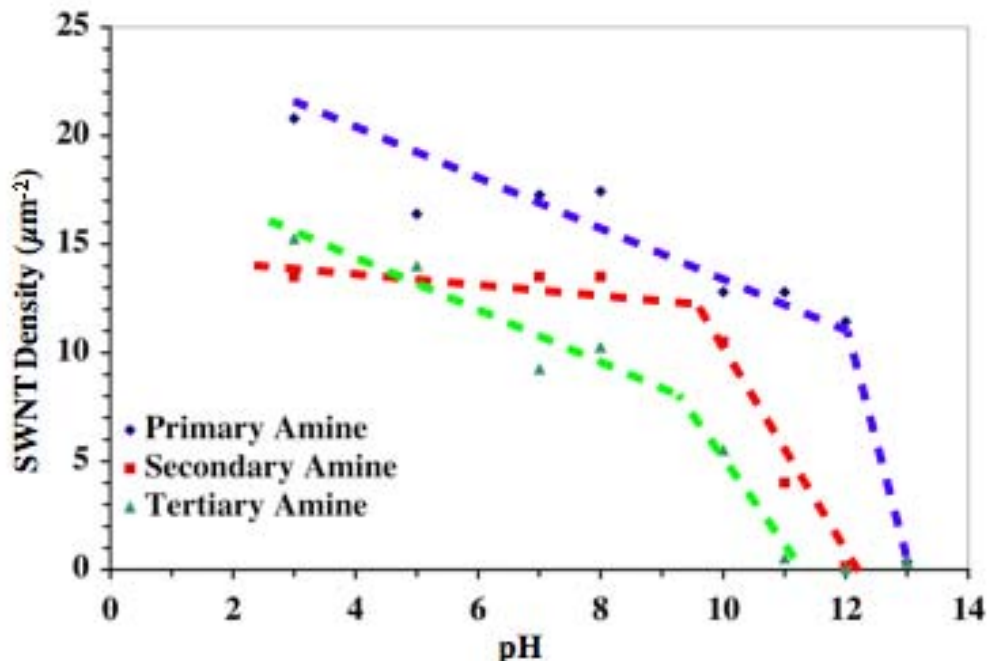


Figure 2: CNT adsorption as a function of bulk solution pH on all three amine surfaces. The nanotube density gradually decreased with increasing pH for all surfaces. Adsorption shutoff took place at decreasing pH as methyl substitution increased. The increased steric hindrance reduced the electrostatic interaction between the SWNTs and the amine, resulting in lower pH values producing adsorption shutoff.

In summary, we have been able to understand the mechanisms of CNT absorption, and use this information to fabricate rationally designed CNT networks from solution with, leading to tunable electronic properties. This is critical for transparent electrodes since the transparency and conductivity metrics are very different for various applications (i.e. solar, displays, touch-screens). Moreover, we are able to integrate these organized films onto plastic surfaces, enabling low-cost large area, flexible transparent electrodes.

IV. Effect of Surface Chemistry on Electronic Properties of Carbon Nanotube Networks

Thin films of single-walled carbon nanotubes (SWNTs) are a viable nanomaterial for next generation sensors, displays, and as electrodes for solar cells. Despite their remarkable properties, due to limitations in synthesis and processing, they have not yet been integrated in current electronics. One of the main challenges is to precisely control the deposition of SWNT films on a variety of surfaces and the understanding of transport properties of these films. We have developed an optimized dry transfer method by which SWNT films can be transferred from a surface that allows for controllable deposition of SWNT films to surfaces that normally do not. By isolating the effect of the surface we gain insight over the fundamental transport properties of SWNT on different surfaces. Thin film transistors (TFT) characteristics, corroborated with μ -Raman spectroscopy, show that by using different surface chemistries, such as with self assembled monolayers (SAMs), it is possible to permanently alter the electronic properties of SWNT films.

V. The Properties of Carbon Nanotubes Dispersed with Semiconducting Polymer

A. Assessing performance of carbon nanotube/P3HT composites under pressure and strain

The nanotube composites for pressure and strain testing were prepared as previously described. We tested weight ratios of 5:1 CNT:P3HT. Two-probe sheet resistance measurements as well as Raman spectral measurements were taken before, during, and after stretching for all samples. As a control group, we also fabricated and tested some pristine CNT samples without any P3HT polymer in solution. Figure 3 shows plots of electrical conductivity versus strain.

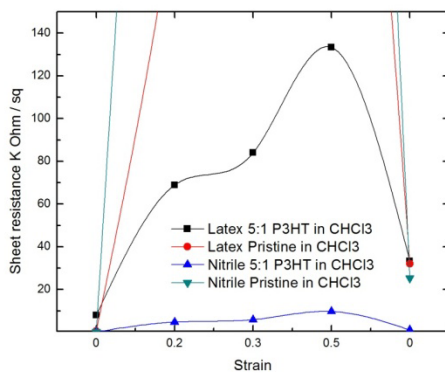


Figure 3: Sheet resistance was plotted versus strain. The black curve represents a 5:1 CNT-P3HT composite in CHCl_3 deposited on a latex substrate. The red curve represents pristine CNT in CHCl_3 deposited on a latex substrate. The blue curve represents a 5:1 CNT-P3HT composite in CHCl_3 deposited on a nitrile substrate. The green curve represents pristine CNTs in CHCl_3 deposited on a nitrile substrate.

In all samples, sheet resistance was found to increase with stretching and to decrease with removal of applied strain. Samples largely but not completely recovered after testing. Pristine CNTs network in CHCl_3 (without adding P3HT) became completely insulating under even small strain.

For vertical pressure response testing, CNT thin films, both without polymer and in a 5:1 CNT:P3HT composite, were deposited on glass slides. A compressive pressure was applied from the vertical direction and the associated sheet resistance change between electrodes was measured. Figure 4 shows the corresponding sheet resistance plotted as a function of vertical compressive pressure for CNT networks deposited on glass substrates. For both pristine samples and 5:1 CNT:P3HT composites, three samples of different tube densities were prepared. During testing, the pressure was raised from 0 to medium pressure (10^2 Pa) to high pressure (10^5 Pa), then decreased to medium pressure and returned to 0. Thus a complete pressure circle was performed, three times for each sample to test reproducibility and reliability.

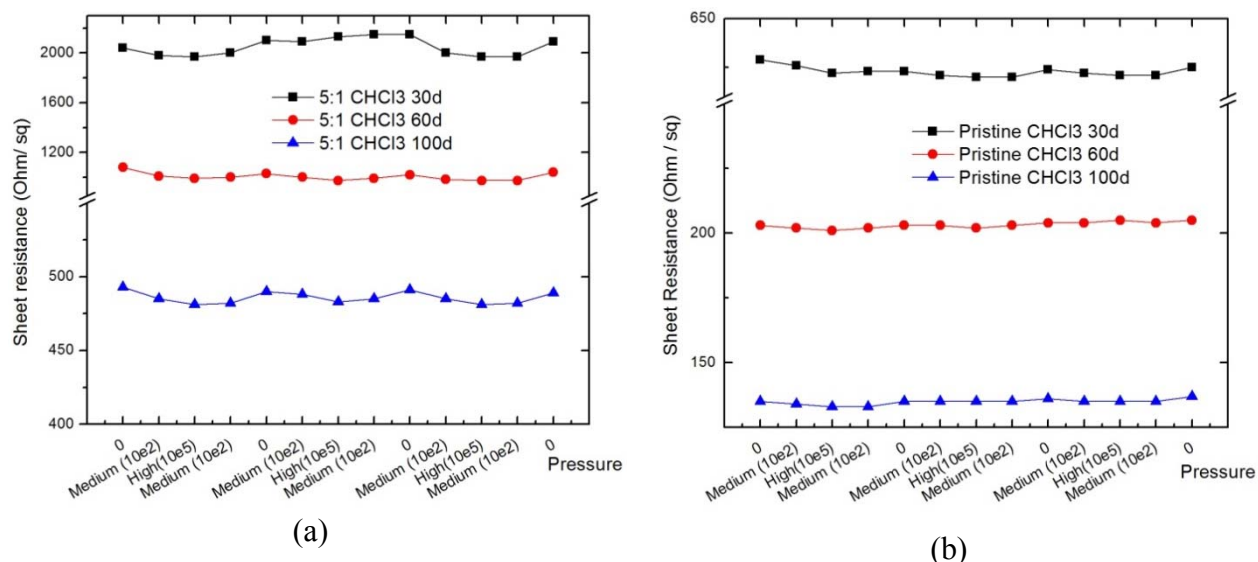


Figure 4: Response of CNT network sheet resistance to vertical pressure. The black, red, and blue curves represent 0.3 ml, 0.6 ml, and 1 ml solution deposited, respectively. **(a)** P3HT was added to CNT solution in a 5:1 weight ratio **(b)** CNT was deposited without polymer.

We observe a clear sheet resistance response to applied pressure. Through each pressure cycle, CNTs sheet resistance decreased with increasing pressure and increased with decreasing pressure. All samples showed a similar trend, but the composites had a much stronger response compared with the pristine samples.

B . Patterning functional carbon nanotube/conjugated polymer composite electrodes directly from solution

In this work, we achieved SWNT and polymer:SWNT composite electrode patterning. After appropriate substrate patterning, the polymer:SWNT composite solution was prepared as in reference 5, and was spin-coated or drop cast onto the substrate. Typical electrode thicknesses were between 20-80 nm, and sheet resistances, calculated by measuring the overall resistance of a patterned electrode and scaling with geometry, were ~1-4 k Ω /sq.

Several example patterned electrode surfaces as imaged by optical microscopy and atomic force microscopy are shown in Figure 5. Since these electrodes were fabricated on opaque substrates, their transparency was not explicitly measured; however, our previous work with similar composite films indicates that they are most likely semitransparent. We have demonstrated that this patterning method can easily produce features as small as 3 microns over areas of more than 3 cm², and there is no indication that these are limiting values. The tube density on a given substrate varies as a function of electrode shape and size on a substrate, indicating that for these selective wetting, rather than selective adhesion, plays the bigger role. As determined by atomic force microscopy, for composite samples tube densities can reach hundreds of tubes/micron within a few hundred nanometers of the pattern edge. Interestingly, we also note that due to the nature of our fabrication method the nanotube bundles at the electrode edge do not predominantly lie perpendicular to that edge. This is in distinct contrast to many previous reports of nanotube-based electrodes for OTFTs, and may have some effect on the role of electric field enhancement in these devices.

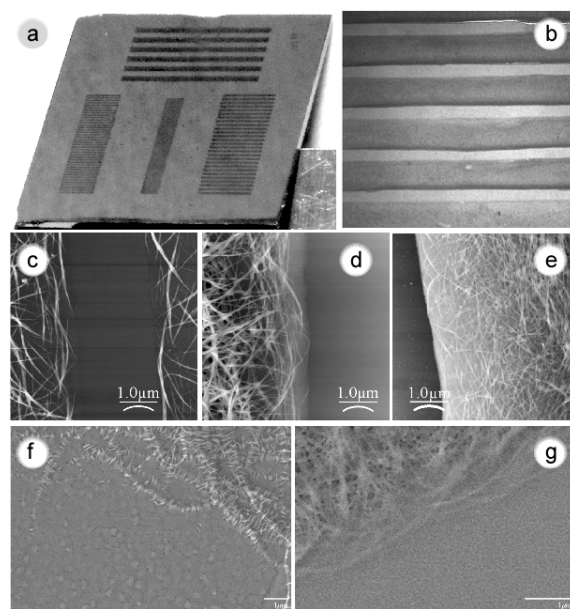


Figure 5. a) A digital photograph of a sample approximately 3 cm² in area, with patterned composite electrodes. b) An optical micrograph (10x objective) of high polymer content (1:1) composite electrodes. Image contrast in a-b has been enhanced for clarity. c) Atomic force micrograph of a patterned 1:1 P3HT:SWNT composite, illustrating successful resolution of 3 micron feature sizes. d) Atomic force micrograph of a patterned 1:1 P3HT:SWNT composite, illustrating a typically achievable tube density gradient. e) Atomic force micrograph of a 1:1 P3HT:SWNT composite deposited on a surface with predeposited Au electrodes. f) Scanning electron micrograph of electrode-semiconductor interface in a polymer:SWNT/pentacene transistor with a thick pentacene layer. g) Scanning electron micrograph of electrode-semiconductor interface in a polymer:SWNT/C₆₀ transistor with a thick C₆₀ layer.

It is well known that the properties of a polycrystalline organic semiconductor thin film depend critically on its morphology, and that the morphology can vary considerably as a function of, among other things, the surface upon which it is grown. Poor morphology at the electrode-semiconductor-dielectric interface has been a prominent difficulty in the development of bottom-contact organic transistors. For this reason we examine the structure of these organic thin films as grown on top of a carbon nanotube network. As the pentacene thickness increases above a few nm (Figure 5f), a film is deposited on the dielectric surrounding the nanotubes, and this film directly abuts the tubes on either side; nevertheless most of the grains on the tubes appear to be disconnected from this broader layer. As with pentacene, C₆₀ selectively nucleates and grows on carbon nanotubes.

Lastly, we characterize the electrical performance of thin-film transistors of pentacene and C₆₀ using these nanotube-based electrodes. All semiconductors were evaporated under high vacuum. Pentacene transistors were tested in air; C₆₀ transistors were tested in a nitrogen-filled glovebox. Over several trials, the saturation-regime mobilities of all devices (channel lengths 50 µm – 150 µm) typically ranged from 0.2-1.5 cm²/V*s.

In conclusion, we developed a method to simultaneously fabricate and pattern carbon nanotube composite electrodes with unprecedented tube densities and excellent feature resolution. We used these electrodes to drive competitive organic transistors. We thereby suggest that this material system and fabrication technique has promise in applications requiring flexible, semitransparent, low-cost complementary circuits.

References:

1. Y. Ito et al., *J. Am. Chem. Soc.*, **2009**, *131*, 9396.
2. A.L. Briseno et al., *Nature*, **2006**, *444*, 913.
3. N. Herzer et al., *Adv. Func. Mater.*, **2009**, *19*, 2777.
4. M.C. LeMieux et al., *Science*, **2008**, *321*, 101.
5. S. Hellstrom et al., *ACS Nano*, **2009**, *3*, 1423.

C. Probing electrical transport in large bundles using nanoscale 4-probe measurements

We have begun a collaborative project with the Center for Nanophase Materials Sciences (CNMS) at Oak Ridge National Lab, TN aimed at better understanding transport through networks of bundled nanotubes, for the purposes of designing better nanotube networks. We deposit sparse networks of bundled tubes from chloroform onto Si substrates with native oxide, and make contact using the 4-probe STM available at CNMS.^[1] We take both two probe measurements scaled along the length of a single bundle, and four probe measurements of single tube bundles and branched tube bundles, as illustrated in Figure 6 We are currently working on data analysis and interpretation, on methods to improve contact between the tubes and the probes, and on measurement consistency.

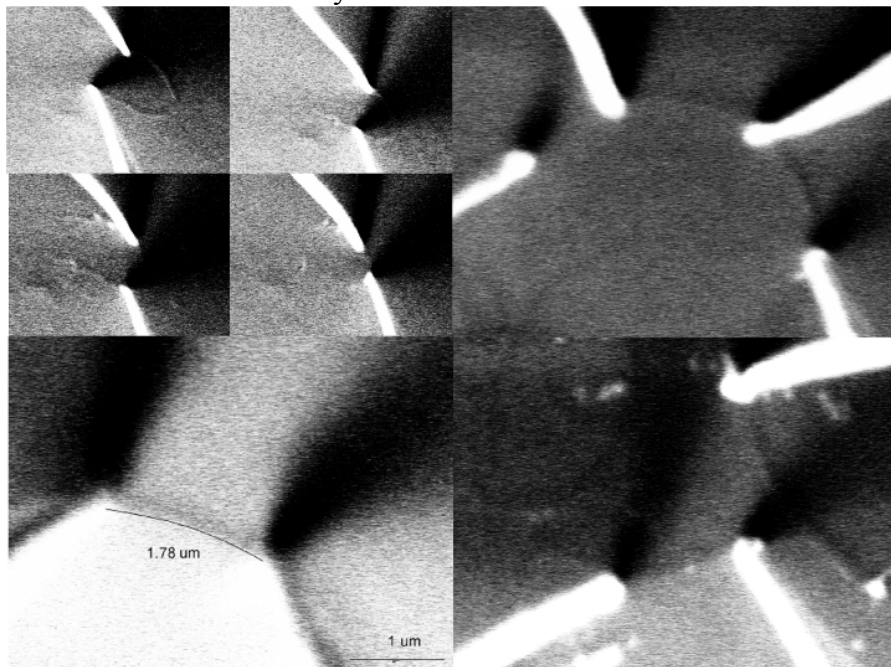


Figure 6: Two and four-probe measurements of nanotube bundles in various configurations.

References:

1. T.-H. Kim et al., *Rev. Sci. Instrum.*, **2007**, *78*, 123701.

Publications:

1. Opatkiewicz, J.P.; LeMieux, M.C.; Bao Z. "Influence of electrostatic interactions on spin assembled single-walled carbon nanotube networks on amine functionalized surfaces", *ACS Nano* 2010, 4, 1167–1177.
2. LeMieux, M.C.; Sok, S.; Roberts, M.E.; Opatkiewicz, J.P.; Liu, D.; Barman, S.N.; Patil, N.; Mitra, S.; Bao, Z. "Solution assembly of organized carbon nanotube networks for thin-film transistors", *ACS Nano* 2009, 3, 4089–4097.
3. Roberts, M.E.; LeMieux, M.C.; Bao, Z. "Sorted and aligned single-walled carbon nanotube networks for transistor-based aqueous chemical sensors", *ACS Nano* 2009, 3, 3287–3293.
4. Roberts, M.E.; LeMieux, M.C.; Sokolov, A.N.; Bao, Z. "Self-sorted nanotube networks on polymer dielectrics for low-voltage thin-film transistors", *Nano Letters* 2009, 9, 2526 – 2531.
5. S.L. Hellstrom, H.W. Lee, Z. Bao, "Polymer-assisted direct deposition of carbon nanotube bundle networks for high performance transparent electrodes", *ACS Nano*, **2009**, 3, 1423.
6. S.L. Hellstrom, R.Z. Jin, R.M. Stoltenberg, Z. Bao, "Driving high-performance n- and p-type organic transistors with carbon nanotube/conjugated polymer composite electrodes patterned directly from solution." *Adv. Mater.*, submitted.
7. Barman, S.; LeMieux, M.C.; Baek, J.; Rivera, R.; Bao, Z. "Solution Processing Single Walled Nanotubes for Rational Design of Network Transistors". Manuscript in progress.
8. Vosgueritchian, M.; LeMieux, M.C.; Bao, Z. "Effect of Surface Chemistry on Electronic Properties of Carbon Nanotube Network Thin Film Transistors". Manuscript in Progress.

Patents:

1. S.L. Hellstrom, H.W. Lee, Z. Bao, #S08-424 (STFD.254PA)
2. M.C. LeMieux, A. Virkar, Z. Bao, # S09-208 (STFD.252PA)

Contact:

zbao@stanford.edu